Review Paper
J. Astron. Space Sci. 41(1), 1-15 (2024)
https://doi.org/10.5140/JASS.2024.41.1.1

JASS Journal of Astronomy and Space Sciences

Long-Term Science Goals with *In Situ* Observations at the Sun-Earth Lagrange Point L4

Dae-Young Lee[1†], Rok-Soon Kim[2], Kyung-Eun Choi[3], Jungjoon Seough[2], Junga Hwang[2], Dooyoung Choi[1], Ji-Hyeon Yoo[1], Seunguk Lee[1], Sung Jun Noh[4], Jongho Seon[5], Kyung-Suk Cho[2], Kwangsun Ryu[6], Khan-Hyuk Kim[5], Jong-Dae Sohn[2], Jae-Young Kwak[2], Peter H. Yoon[7]

[1]Department of Astronomy and Space Science, Chungbuk National University, Cheongju 28644, Korea
[2]Space Science Division, Korea Astronomy and Space Science Institute, Daejeon 34055, Korea
[3]Space Sciences Laboratory, University of California, Berkeley, CA 94720, USA
[4]ISR-1: Space Science and Applications, Los Alamos National Laboratory, Los Alamos, NM 87545, USA
[5]Department of Astronomy & Space Science, College of Applied Sciences, Kyung-Hee University, Yongin 17104, Korea
[6]Satellite Technology Research Center, KAIST, Daejeon 34141, Korea
[7]Institute for Physical Science and Technology, University of Maryland, College Park, MD 20742, USA

The Korean heliospheric community, led by the Korea Astronomy and Space Science Institute (KASI), is currently assessing the viability of deploying a spacecraft at the Sun-Earth Lagrange Point L4 in collaboration with National Aeronautics and Space Administration (NASA). The aim of this mission is to utilize a combination of remote sensing and in situ instruments for comprehensive observations, complementing the capabilities of the L1 and L5 observatories. The paper outlines long-term scientific objectives, underscoring the significance of multi-point in-situ observations to better understand critical heliospheric phenomena. These include coronal mass ejections, magnetic flux ropes, heliospheric current sheets, kinetic waves and instabilities, suprathermal electrons and solar energetic particle events, as well as remote detection of solar radiation phenomena. Furthermore, the mission's significance in advancing space weather prediction and space radiation exposure assessment models through the integration of L4 observations is discussed. This article is concluded with an emphasis on the potential of L4 observations to propel advancements in heliospheric science.

Keywords: Sun-Earth Lagrange point L4, solar wind, *in situ* observations, space weather, space radiation

1. INTRODUCTION

The Korean heliospheric community, led by the Korea Astronomy and Space Science Institute (KASI) and supported by the Korean government, is currently engaged in a feasibility study in collaboration with a National Aeronautics and Space Administration (NASA) group to explore the possibility of siting a spacecraft at the Sun-Earth Lagrange point L4. This initiative involves a spacecraft equipped with various remote-sensing and in situ instruments, as outlined in the studies by Cho et al. (2023). The strategic placement of the spacecraft at L4, which is located 60° ahead of Earth in orbit, offers distinct advantages, particularly when integrated with other space observatories positioned at L1 and L5 (Posner et al. 2021).

At Lagrange Point L1, NASA plans to deploy the Space Weather Follow On Lagrange 1 (SWFO-L1), slated for launch as a rideshare with NASA's Interstellar Mapping and Acceleration Probe (IMAP) mission in 2025 (https://www.nesdis.noaa.gov/next-generation/space-weather/

This is an Open Access article distributed under the terms of the Creative Commons Attribution Non-Commercial License (https://creativecommons.org/licenses/by-nc/3.0/) which permits unrestricted non-commercial use, distribution, and reproduction in any medium, provided the original work is properly cited.

Received 29 DEC 2023 **Revised** 20 JAN 2024 **Accepted** 22 JAN 2024
†**Corresponding Author**
Tel: +82-43-261-2316, E-mail: dylee@chungbuk.ac.kr
ORCID: https://orcid.org/0000-0001-9994-7277

swfo-instruments). Additionally, the European Space Agency (ESA) is contemplating the siting of another spacecraft, named Vigil, at L5. Vigil is designed to offer advanced warning of solar storms, providing valuable time for enhanced space weather prediction efforts (https://www.esa.int/Space_Safety/Vigil; https://space.oscar.wmo.int/satellites/view/vigil_l5).

As introduced in Cho et al. (2023), in situ measurements of the L4 mission will be conducted by means of various instruments, including a solar wind plasma analyzer, high-energy particle detector, fluxgate and search coil magnetometers, radiation monitor, radio/wave detector, and dust detector. By combining in situ observational data from these instruments with remote sensing observations, as well as data from L1 and L5, we anticipate significant scientific advancements and breakthroughs in various key research areas.

The aim of this paper is to provide a comprehensive overview of major science topics, primarily leveraging the anticipated in situ observations at L4, complemented by data from L1 and L5. The objective is to assist and guide the ongoing feasibility study conducted by KASI. Recognizing that the launch of the L4 spacecraft is anticipated to be 10 years or later, we have chosen to prioritize science topics that necessitate long-term research efforts. We endeavor to actively identify and organize research topics, primarily led by researchers in the Korean heliospheric community, alongside their international colleagues. However, we acknowledge the possibility of unintentionally overlooking emerging research topics in the future.

2. LONG-TERM SCIENCE ISSUES

2.1 Large-Scale Phenomena and Structures

Conducting in situ observations at L4 is expected to enhance our understanding of large-scale phenomena and structures in the solar wind, particularly when integrated with observations at L1 and L5. Here, we have chosen three specific subjects, which stand to gain valuable insights from observations at multiple Lagrangian points.

2.1.1 Coronal Mass Ejections

Coronal mass ejections (CMEs) are the primary cause of geomagnetic storms, which has made them a consistent and enduring focus of significant research efforts. As they propagate through the heliosphere, they continually interact with the ambient solar wind, leading to their speeds generally decelerating or occasionally accelerating (e.g., Vršnak & Gopalswamy 2002; Vršnak 2006). This interaction can impede our ability to predict the arrival time of CMEs and associated shocks at Earth (e.g., Kim et al. 2007). By tracking CME propagations and eventually directly confirming the interplanetary coronal mass ejection (ICME) arrival at 1 AU, we can obtain more precise insights into CME acceleration and deceleration. Coordinated observations at L1 and L4 can certainly enhance progress toward this scientific goal. Fig. 1 illustrates remote sensing observations at L1 and in situ observations at L4 for a CME event. Such coordinated observations are also crucial for understanding other significant CME-related issues, including structural deformation after CME-CME interactions (e.g., Scolini et al. 2020) and the extended sheath and shrunken magnetic clouds following interactions with the solar wind.

CMEs, and eventually ICMEs, undergo continuous evolution in both temporal and spatial dimensions (Kim et al. 2013). Despite long-term continuous observations at L1, single-point observations have limitations in fully understanding the structure and evolution of ICMEs. It is clearly desirable to have multiple-point observations with proper alignment of the observing spacecraft (see examples in Fig. 2). Placing a spacecraft at L4 and coordinating with L1 and L5 should fulfill such scientific goals to some extent. As inferred in Fig. 2, a radial alignment of multiple spacecraft (green) is useful for understanding the temporal evolution of CME rotations, deflections, etc., while a longitudinal alignment of spacecraft (red), such as at the three Lagrange points, can help clarify the spatial structure of ICMEs, thereby increasing the reliability of magnetic cloud modeling (further discussed below). Without a specific alignment (black), distinguishing between the radial and longitudinal dependencies of ICME properties is challenging.

Multipoint observations should offer an integrated view of the cross-sectional structure of ICMEs, a precision

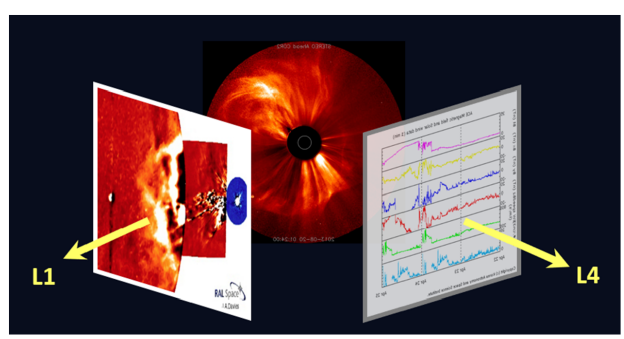

Fig. 1. Demonstration of remote sensing observations at L1 and *in situ* observations at L4 for the same CME event. CME, coronal mass ejections.

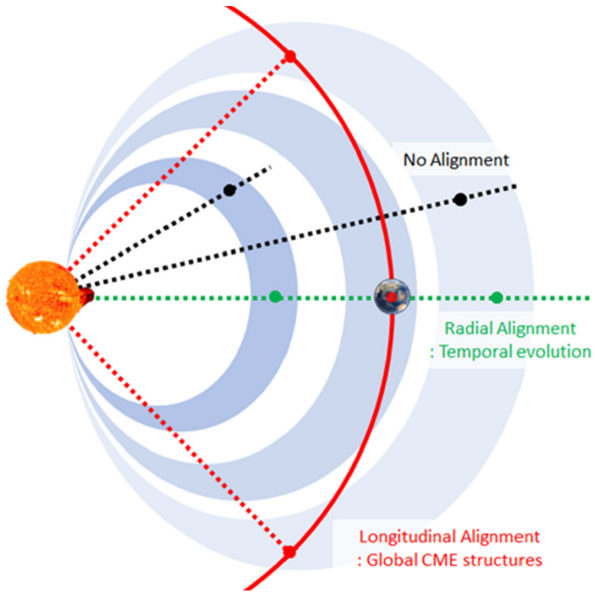

Fig. 2. Comparison scenarios of multi-spacecraft alignment for CME observations: radial alignment (green), longitudinal alignment at the three Lagrangian points (red), and no specific alignment (black). CME, coronal mass ejections.

not achievable by a single spacecraft, as demonstrated in Gopalswamy (2006) and Kim et al. (2013). This approach will facilitate the determination of the global magnetic flux rope structure of ICMEs in a more accurate manner. Ultimately, it will contribute to predicting the precise ICME structure that interacts with Earth's magnetosphere, thereby enhancing the reliability of space weather predictions.

2.1.2 Magnetic Flux Ropes of Mesoscale

ICMEs often exhibit a distinct large-scale structure in the form of a magnetic flux rope known as a magnetic cloud. A similar flux rope structure on a mesoscale (Viall et al. 2021), considerably smaller than the scale of magnetic clouds but still larger than the kinetic scale, has been regularly observed at nearly all heliospheric distances, irrespective of the sunspot cycle phase (e.g., Chen & Hu 2020; Choi et al. 2021; Chen et al. 2023). These structures are referred to as small-scale magnetic flux ropes (SMFRs). The spatial scale of SMFRs is typically one-tenth that of magnetic clouds when observed at 1 au. In contrast to the extensive history of typical magnetic cloud research, SMFR research has a relatively shorter history, and our understanding of these clouds is still limited, necessitating sustained and intensive research. Currently, the origin and specific structure of such SMFRs are active research subjects in the heliospheric science community, in which both solar origins due to small ejecta or reconnections near helmet streamer tips and interplanetary origins due to reconnections and turbulence are considered (e.g., Rouillard et al. 2011; Zheng & Hu 2018; Choi et al. 2022, 2024). Moreover, SMFRs are closely associated with switchbacks which are characterized by local short-term deflections of the magnetic field (e.g., Jagarlamudi et al. 2023). These switchbacks have been frequently observed by the Parker Solar Probe in close proximity to the Sun and, at other outer heliospheric distances, by spacecraft such as Helios, WIND and Ulysses (e.g., Horbury et al. 2018). Investigating the precise relationship between SMFRs and switchbacks is a subject of intense research (e.g., Drake et al. 2021).

Given the high detection rate inferred from numerous single spacecraft observations, there is no reason to preclude the possibility of the near-simultaneous existence of more than one SMFR at different locations. Comparing such SMFRs at two or three Lagrange points presents a compelling avenue for advanced research. SMFRs are typically well distinguished from higher-density background solar wind and are often referred to as blobs (as shown in Fig. 3). Spacecraft at different Lagrange points can encounter SMFRs in various ways, as depicted in Fig. 3, which illustrates a set of possible scenarios for satellite crossings through SMFRs and the corresponding background (Sanchez-Diaz et al. 2019).

Recent investigations, drawing on comparisons between observations at different heliospheric distances, such as those from the Parker Solar Probe in close proximity to the Sun and those at 1 AU by WIND, reveal that while large-scale heliospheric current sheets (HCS; discussed below) remain largely consistent, small-scale structures such as flux ropes and blobs exhibit significant differences (Szabo et al. 2020). This suggests a noteworthy evolution in the inner heliosphere that is potentially influenced by the longitude.

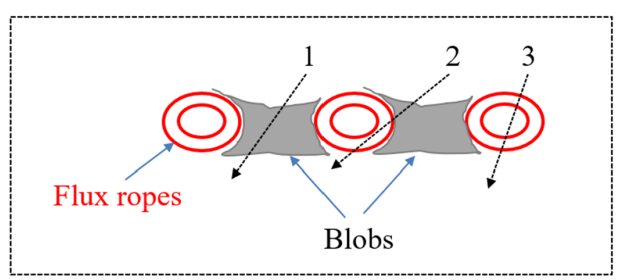

Fig. 3. Scenarios for the potential passage of spacecraft through flux ropes (depicted in red) and the corresponding background high-density region, blobs (represented by the gray area). In Scenario 1, the spacecraft will not detect a flux rope; in Scenario 2, it will encounter the blob region first, followed by the flux rope; and in Scenario 3, the spacecraft will observe the flux rope only. Adapted from Sanchez-Diaz et al. (2019) with American Astronomical Society.

A challenging yet promising endeavor would involve comparing small-scale structures, such as SMFRs, among different longitudinal points (the three Lagrange points), coupled with a radial comparison, to comprehensively understand the evolution of SMFRs.

2.1.3 Heliospheric Current Sheets

The HCSs are an interplanetary extension of the solar neutral line (Schulz 1973). HCSs can be warped (Jokipii & Thomas 1981), and the degree of warping depends on the solar cycle phase. Consequently, the likelihood of a spacecraft encountering HCSs at high latitudes increases when warping is significant, a phenomenon typically observed near the solar cycle maximum, as illustrated in Fig. 4 (Hoeksema et al. 1983).

Moreover, the HCS structure is intricate due to variations in the orientation (or local tilt angle), a broad range of thickness [from ~100s km to ~10^6 km (~7×10^{-3} au)], the potential existence of multiple current sheets, and the distortion and reformation caused by propagating ICMEs (Jokipii & Thomas 1981; Winterhalter et al. 1994; Lepping et al. 1996; Smith 2001; Blanco et al. 2008; Neugebauer 2008; Liou & Wu 2021). The radial dependence of the HCS has been previously investigated, including examinations at distances very close to the Sun based on Parker Solar Probe observations (Lavraud et al. 2020; Szabo et al. 2020) and at far distances in the inner heliosheath (Burlaga et al. 2018; Choi et al. 2023). However, there is a notable scarcity of research on the longitudinal dependence of HCSs, and our current understanding of this aspect is relatively limited. As depicted in Fig. 5, observations from multiple Lagrange points may reveal diverse structures of the HCS, if identified, thereby contributing to a more comprehensive understanding of these complex issues.

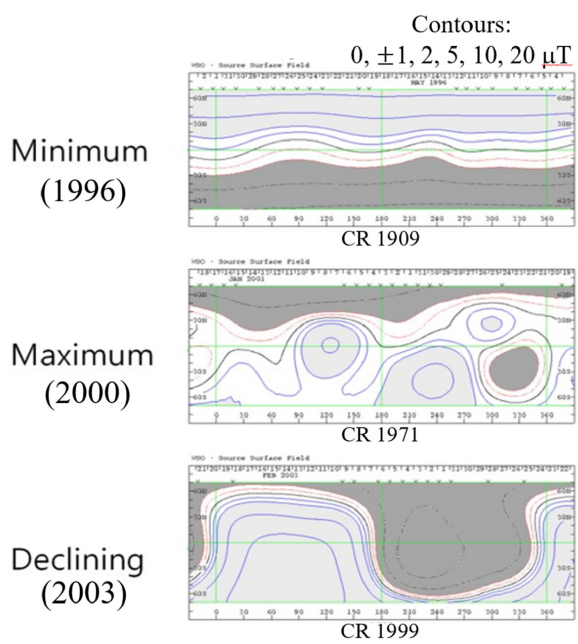

Fig. 4. Contours of the magnetic field intensity and the neutral line at the source surface of 2.5 $R_{\odot}$, obtained from the Potential Field Source Surface model, for three selected Carrington rotation times, each corresponding to a different solar cycle phase. Adapted from Wilcox Solar Observatory (2023) with permission of author.

2.2 Suprathermal and Energetic Particles

Suprathermal and energetic particles constitute crucial elements in the L4 mission. The forthcoming spacecraft is equipped with in situ instruments dedicated to the study of these particles, facilitating a diverse range of research. Along with remote sensing at L4, coordinated observations at multiple Lagrangian points will significantly amplify the benefits derived from investigating these particles.

2.2.1 Suprathermal Electrons

Suprathermal isotropic halos and field-aligned strahl electrons constitute approximately 4%–10% of the solar wind electron population. Notably, strahl beams are instrumental in determining magnetic field geometry, indicating whether the field is open, closed, or disconnected (Owens & Forsyth 2013). These beams are most effectively

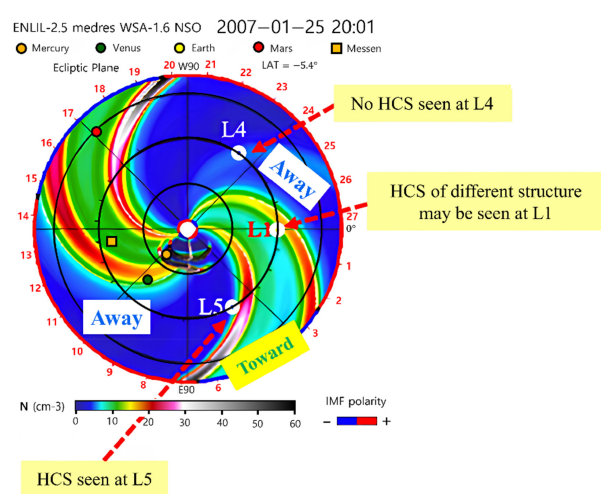

Fig. 5. A scenario depicting the HCS structure across a spatial scale of approximately 120 degrees in longitude, incorporating observations from three Lagrange points. In this specific instance, the spacecraft at L1 and L5 are positioned at the sector boundaries, while there is no sector boundary at L4. Note that the sector polarities are denoted by red and blue encircling the circle. HCS, heliospheric current sheet.

observed/identified at typically 100s eV and are often broad, possibly due to interactions with plasma waves such as whistler waves (Pagel et al. 2007; Cattell & Vo 2021). While bi-directional beams generally suggest a closed field line geometry, complications can arise due to the presence of local field enhancements, primarily associated with co-rotating interaction regions (CIRs) and interplanetary shocks ahead of ICMEs (Choi et al. 2021). Fig. 6 illustrates how such situations can occur, and diverse situations may be encountered through observations at different Lagrange points.

The electron strahl beams can be used to determine the true sector boundary (TSB) between heliospheric magnetic polarity changes, signifying that the strahl beam direction switches from parallel propagation to antiparallel propagation (or vice versa) along the magnetic field lines in each hemisphere (Lavraud et al. 2020). While this principle suggests the co-location with the HCSs, in reality, they are not necessarily consistent with each other. Since the HCS can be defined from the magnetic field polarity reversal, more than one current could exist within a broader HCS layer. Fig. 7 illustrates a possible scenario where the interchange reconnection between an initially closed loop and an open field line creates the HCS, while the true sector boundary defined by the strahl beam directions is located somewhat differently. Such interchange reconnection-generated loops are transient and evolve over time, and spacecraft at different positions, such as L4 and the other Lagrange points, may encounter different structures of the HCS and true sector boundary. Hence, a meticulous analysis incorporating both suprathermal electron and magnetic field data is essential for obtaining a clear and unambiguous distinction between the TSB and the HCSs.

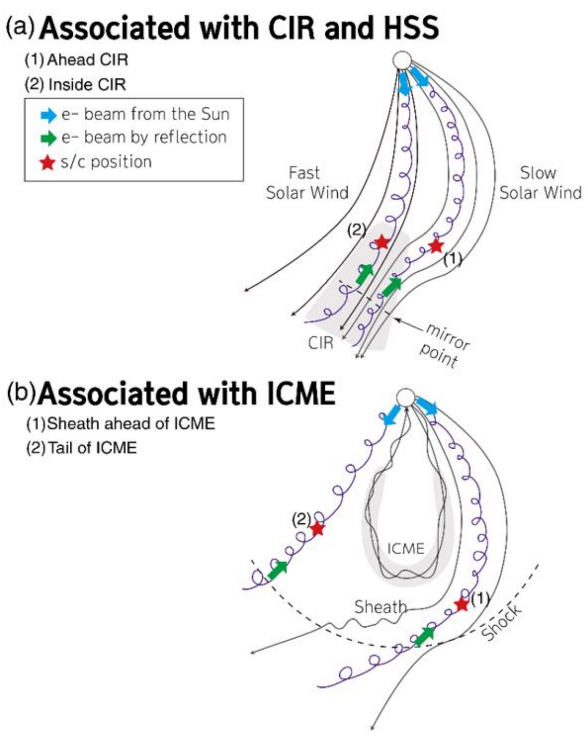

Fig. 6. Schematic demonstration of reflections (green arrows) of originally anti-sunward strahl beams (blue arrows) due to (a) a locally enhanced magnetic field in the CIR region and (b) ICME-driven shock. The spacecraft (red star) can observe bi-directional strahl beams even though the field lines are open. Adapted from Choi et al. (2021) with CC-BY. CIRs, co-rotating interaction regions; HSS, high speed stream; ICME, interplanetary coronal mass ejection.

2.2.2 Solar Energetic Particles

Intense solar energetic particles (SEPs), as highlighted by Desai & Giacalone (2016), can potentially cause substantial radiation harm to humans during space exploration, particularly as we approach the era of lunar and Mars exploration (Cucinotta et al. 2010). The risk of radiation exposure to astronauts in space primarily stems from SEP events involving protons of approximately 50 MeV. The significance of the L4 mission lies in its pivotal role in predicting and forecasting these hazardous radiation risks, extending beyond mere academic interest and directly impacting the safety of astronauts.

While CMEs propagate in a near-radial fashion from the Sun to 1 AU and beyond, the movement of energetic particles is generally guided by magnetic fields within the heliosphere. Notably, at 1 AU from the Sun, particularly near

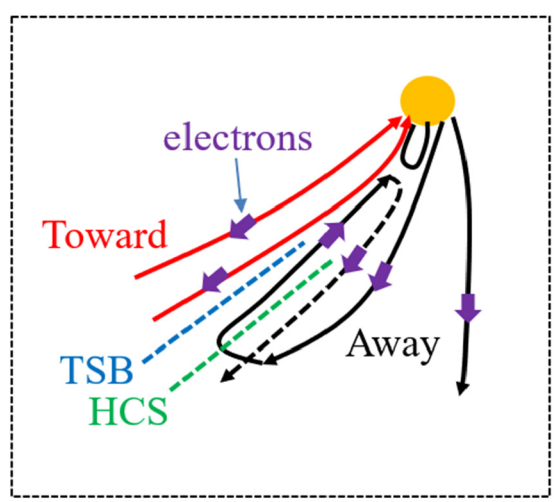

Fig. 7. An illustrative scenario showing the distinction between the true sector boundary (TSB) and the heliospheric current sheet (HCS). The TSB is defined based on the strahl beam flow directions relative to the background magnetic field, in contrast to the HCS, which is defined by local changes in magnetic field polarity. Adapted from Foullon et al. (2009) with Springer Nature.

the ecliptic plane, SEPs are magnetically linked to flares/CMEs originating ~60° west of the Sun (Posner et al. 2021), an area ideally observable by the L4 mission. Additionally, Richardson et al. (2014) documented that approximately 30% of the most hazardous SEP events during the two-STEREO era originated behind the western solar limb relative to a 1 AU observer, including Earth. However, there is a scarcity of observations of flares occurring behind the western solar limb. Observations from the L4 mission will provide crucial data for refining models and predictions (further discussed below) related to space weather, particularly SEPs, which are vital for safeguarding human activities and assets in space.

Conventionally, two kinds of SEPs are considered (e.g., Reames 2020). Impulsive events are those caused by flares associated with impulsive Hα and X-ray flares or jets for short durations (~several hrs.). They mostly occur in the western region, which is magnetically well connected to Earth. These events are ^{3}He-rich and frequently accompanied by type III radio bursts, the ideal tracer of energetic electron escape from the magnetic reconnection site. Particle acceleration in impulsive events starts from lower energy levels [as shown in Fig. 8(a)], progressing rapidly to high energies within a short timescale (Miller et al. 1990; Kim et al. 2014). Gradual events are those caused by CME-driven shocks and are associated with fast CMEs for long durations (~several days), covering a broad longitudinal range. These events are proton-rich and often accompanied by type II radio bursts caused by interplanetary shocks. As shown in Fig. 8(b) (Kim et al. 2014), particle acceleration in gradual events starts from higher energy levels, and low-energy particles arise later as the shock propagates further into the solar wind (Zank et al. 2000).

Traditionally, a clear distinction between two types of SEPs is evident in their spatial extent. Impulsive events are typically observed over a narrow range of heliographic longitudes due to the spatially compact acceleration region. In contrast, gradual events are typically observed over a broader range in longitude, as the injection of accelerated particles occurs on magnetic field lines spanning a wider longitudinal range as the shock intersects these lines near the Sun. Exceptional cases exist, indicating that individual impulsive SEP events were observed at multiple spacecraft situated across a longitudinally broad range (Reames et al. 1991; Wiedenbeck et al. 2010, 2013). Clearly, understanding the longitudinal dependence of flare-accelerated particles requires multiple spacecraft observations. Additionally, time delays in SEP onset and peak intensity increase with an increasing connection angle between the solar event and the foot points of the magnetic field lines passing through the observing spacecraft (Richardson et al. 2014). Therefore, in situ observations at multiple Lagrange points, including L4, should play a vital role in resolving all these issues.

2.3 Kinetic-Scale Sciences and Their Relationship to Large-Scale Aspects

The L4 mission can extend its benefits to kinetic-scale sciences, including kinetic plasma waves and instabilities

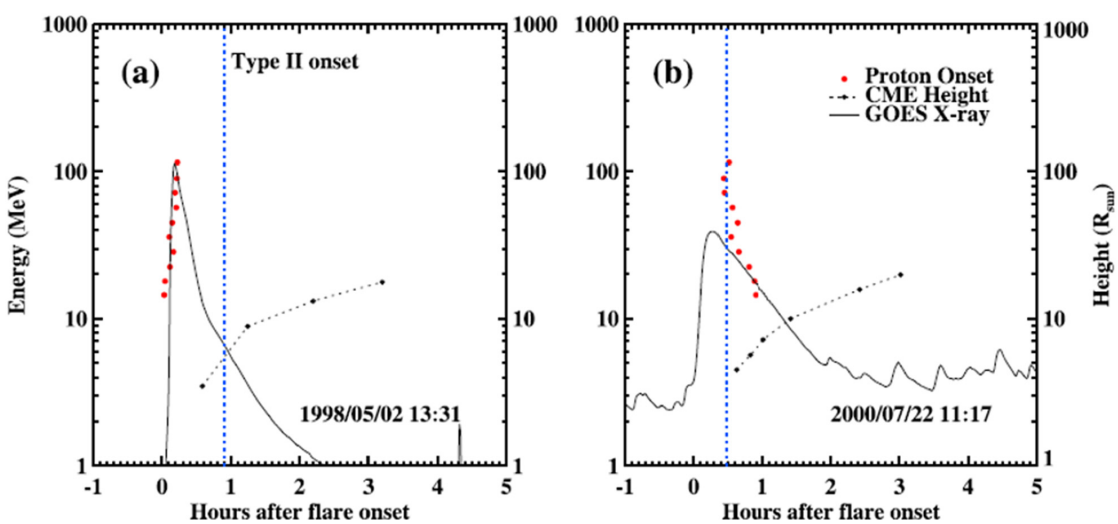

Fig. 8. Comparison of the SEP onset time dependence on energy (red dots) between impulsive (a) and gradual (b) SEP events. The associated flares, CMEs, and IP type II radio bursts are also shown for reference. Adapted from Kim et al. (2014) with CC-BY-NC-ND. SEP, solar energetic particles; CME, coronal mass ejections.

that are locally excited but may propagate on a large scale. SEPs serve as the origin of some solar radio bursts, acting as a proxy for early warnings of energetic events originating in proximity to the Sun. The intricate connection between solar radio bursts and nonlinear plasma physics at the kinetic scale further underscores the mission's significance.

2.3.1 Kinetic Waves/Instabilities

A series of studies has reported widespread observations of enhanced magnetic fluctuations near proton/electron cyclotron frequencies in the inner heliosphere (Jian et al. 2009; Breneman et al. 2010; Lacombe et al. 2014; Boardsen et al. 2015; Gary et al. 2016; Stansby et al. 2016; Bale et al. 2019; Zhao et al. 2019; Tong et al. 2019; Agapitov et al. 2020; Bowen et al. 2020; Cattell et al. 2020; Verniero et al. 2020; Liu et al. 2023). These electromagnetic waves at the ion/electron scale include Alfven ion cyclotron, fast magnetosonic, and whistler waves, and they are believed to play a crucial role in heating, accelerating, scattering coronal and solar wind plasma particles and regulating heat flux in solar wind through wave-particle resonant interactions (Pagel et al. 2007; Cattell & Vo 2021; Bowen et al. 2022; Squire et al. 2022; Raouafi et al. 2023). While many issues concerning the origin of such kinetic-scale waves are still debated, recent observations suggest that these waves could be locally generated in an interplanetary medium through plasma kinetic instabilities (Gary et al. 2016; Liu et al. 2023). Despite the well-known fact that velocity space micro-instabilities arise when the plasma deviates far from thermal equilibrium, the underlying physical mechanisms giving rise to the non-thermal features of particle velocity distributions observed in the inner heliosphere remain unclear.

Crucially, multi-scale coupling between global solar wind expansion and local kinetic processes governs the dynamic and thermodynamic evolution of solar wind plasma (Verscharen et al. 2019; Seough et al. 2023). These complex interactions can be traced through both in situ measurements of local plasma properties (for small-scale processes) and remote sensing observations of the origin of global structures (for large-scale processes). These fluctuations may result in a concomitant variation in the particle velocity distribution, consequently generating plasma waves at kinetic scales. In-situ observation data from L4, along with data from other Lagrangian points, should enhance our comparative understanding of kinetic nature among different locations. This approach is valuable for clarifying the aspects in which kinetic physics differs at various longitudinal locations in comparison with differences in the radial direction, a topic that has been extensively studied.

The impact of kinetic-scale waves on solar wind particles is notable not only due to their intensive and brief interactions, as elucidated by linear/nonlinear processes (Bowen et al. 2022) but also due to their extended lifespan (Telloni 2021). While most of these waves, induced by kinetic instabilities, are believed to originate in the inner heliosphere (Jian et al. 2009; Jagarlamudi et al. 2021; Liu et al. 2023), observations of the solar wind near Earth consistently reveal the presence of these waves at 1 AU. Additionally, a meticulous analysis of the observed wave properties indicates that certain waves detected at 1 AU are generated and propagate from as close as 0.56 AU (Wei et al. 2016). The remarkable longevity of kinetic waves holds the potential to significantly influence macroscopic solar wind changes. To comprehensively investigate wave propagation on a large scale, collaborative efforts within the heliophysics community are essential. Utilizing data from inner heliospheric missions, including the Parker Solar Probe, Solar Orbiter, and BepiColombo missions, holds the potential to yield valuable insights. Furthermore, the expanded coverage at 1 AU, facilitated by missions such as L4, along with missions at L1 and L5, will enhance opportunities for in-depth conjugate research in this field.

2.3.2 Solar Radio Bursts: Proxies for Early Warning and Unraveling Nonlinear Plasma Physics

As already alluded to in Section 2.2, it is commonly accepted that type III radio bursts result from energetic electrons associated with impulsive SEP events generated during a solar flare, while type II radio bursts are related to CMEs and gradual SEP events (Reames 2013, 2023). Consequently, the detection of solar radio bursts, encompassing both type II and III bursts (Melrose 2017), is closely tied to the early warning aspects of SEP events. Notably, type III bursts are of particular value as they originate at solar atmospheric altitudes where geo-effective disturbances are most likely to occur. As such, they could serve as a proxy for early warning of energetic events (White 2007). Obviously, having an L4 satellite equipped with a suitable radio antenna to detect these electromagnetic emissions could greatly improve space weather prediction capabilities.

Beyond these pragmatic considerations, the study of solar radio bursts, particularly type III bursts, and, to a certain extent, type II bursts, is important from the perspective of fundamental plasma physics. The basic radio emission mechanism, known as "plasma emission" (Ginzburg &

Zheleznyakov 1958; Melrose 1980; MacLean & Labrum 1985), has played the role of a testbed for nonlinear plasma theory, resulting in a recent comprehensive comparative analysis between theoretical predictions and computer simulations (Lee et al. 2019). However, the existing works relate to plasma conditions typical of the interplanetary space characterized by a high ratio of plasma-to-gyrofrequency, i.e., the "unmagnetized plasma" condition. For radio sources close to solar atmospheric altitudes where geo-effective disturbances originate, the assumption of "unmagnetized" plasma may no longer be valid (Morosan et al. 2016). For such a situation, an entirely new nonlinear theory of plasma emission must be formulated. While simulation efforts have recently started to tackle this issue (Lee et al. 2022), addressing this issue through theoretical endeavors constitutes a challenge for the future. An improved plasma emission theory for a magnetized plasma environment could, in turn, help improve the early warning aspects of geo-effective disturbances, for instance, by providing a better model for radiation characteristics such as wave polarization and beaming angle.

2.4 Modeling with Data from L4 Measurements

The L4 mission has the potential to significantly enhance space weather prediction modeling, covering various aspects, such as CMEs, energetic particles, magnetic flux ropes, space radiation, and solar wind speed and density, over a broad longitudinal range. In situ measurements conducted by the L4 spacecraft will undoubtedly contribute to refining the capabilities of these models.

2.4.1 Models for Determining the CME Evolution and Associated Particle Acceleration

Multiple-point observations should enhance our ability to reconstruct the propagation and evolution of CME and model particle acceleration processes (e.g., Palmerio et al. 2022). Conventional solar wind propagation models include coronal models (such as the WSA and EUHFORIA-corona), CME models (such as cone, spheromak, torus, and FRi3D), and heliosphere models (such as the Enlil and EUHFORIA-heliosphere models) (Odstrcil 2003; Sheeley 2017; Pomoell & Poedts 2018). Particle acceleration models, such as SEPMOD and PARADISE, have been utilized in the community [see Whitman et al. (2023) for a comprehensive review and related references]. To enhance the performance of such models, higher-resolution input parameters and data assimilation at as many points as possible are needed. As depicted in Figs. 1 and 2 in Wijsen et al. (2019), at the location of the cyan symbol, the cutoff in the particle intensity becomes more gradual due to cross-field diffusion, while at the location of the orange symbol, the effect of cross-field diffusion is to shift the particle onset to an earlier time (right panel). This highlights that the SEP event is a local phenomenon dependent on longitude. Consequently, the accuracy and details of SEP predictions should vary with longitudinal distance from the corresponding CME eruption point. To enhance the performance of such models, continuous multi-point observations combined with appropriate data assimilation methods are indispensable.

2.4.2 Flux Rope Modeling

Conventionally, interplanetary magnetic flux ropes have been modeled using force-free fitting for low-β (β = the ratio of plasma to magnetic pressure) plasma cases (e.g., Moldwin et al. 1995). The Grad-Shafranov reconstruction is a useful tool for arbitrary β plasma cases (e.g., Zheng et al. 2017), and other researchers have employed magnetic helicity-based techniques to identify flux ropes in solar wind (e.g., Telloni et al. 2012; Zhao et al. 2020). Fig. 9 shows an example where the flux rope is modeled by both force-free fitting and Grad-Shafranov reconstruction since the plasma

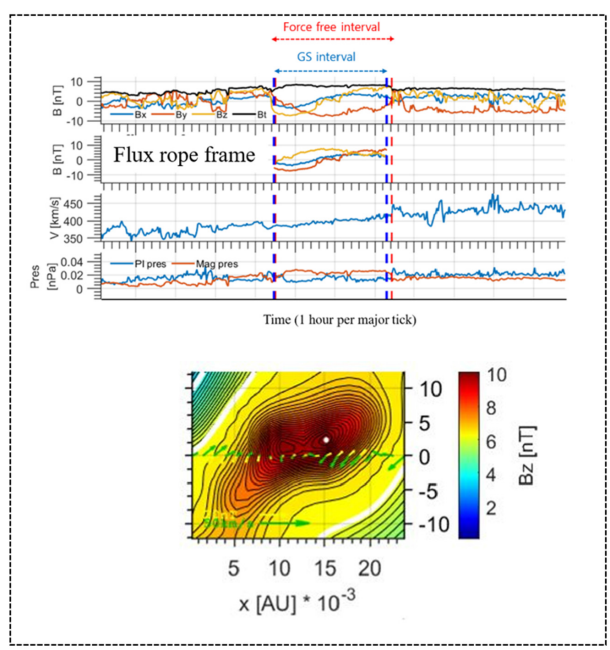

Fig. 9. Example of a magnetic flux rope structure modeled using the Grad-Shafranov reconstruction technique (applied to the interval between the blue vertical lines), with a cross-sectional view of the flux rope surface (lower panel). The force-free fitting technique was successfully applied to the interval between the red vertical lines. The data at the upper panels refer to in situ observations of the magnetic field, solar wind bulk speed, and plasma and magnetic pressures.

β is low in this event. Spacecraft at different locations may observe different structures of flux ropes due to evolution during propagation and/or possible longitudinal structures. A comparison of the modeling results for a flux rope event at L4 with those at other positions can certainly enhance our understanding of the spatial and temporal structure of flux ropes. From a technical viewpoint, comparing modeling results among different methods is challenging and requires continuous effort.

2.4.3 Space Radiation Model

Recently, there has been an increasing necessity for more precise prediction and measurement of aviation radiation in Korea. In the interest of ensuring the radiation safety of our aircrew and passengers, KASI and the Korea Meteorological Administration-National Meteorological Satellite Center (KNMSC) jointly developed their own radiation prediction model, named the Korean Radiation Exposure Assessment Model for the aviation route dose (KREAM) (Hwang et al. 2010, 2014). KREAM is a physics-based aviation radiation dose calculation program designed for altitudes of 0–80 km that incorporates physical models such as GEANT4 and NRLMSIS00 and a cutoff rigidity model (refer to Fig. 10). KREAM utilizes input energy spectra from both galactic cosmic rays (GCRs) and SEPs. SEP information from real-time proton data observed in geosynchronous orbit is integrated into KREAM. Currently, KREAM calculates the effective radiation dose rate to which humans are exposed at aviation altitudes. In the near future, KASI plans to expand the radiation prediction capabilities of KREAM to far higher altitudes, extending into deep space. By incorporating SEP protons at the L4 location, earlier than geosynchronous orbit, the prediction model can work with a longer preceding time, enhancing its usefulness. Furthermore, this extension will cover predictions for low Earth orbit and beyond. The radiation flux/fluence data support the evaluation and prediction of Single Event Effects (SEEs) and total ionization dose (TID) during space missions, including low Earth orbit (Sinclair & Dyer 2013). Calculating the estimated total ionizing dose for a satellite's lifetime during the manufacturing period is crucial (Hughes & Benedetto 2003). The extended version of KREAM can be used to estimate radiation exposure for both manned and unmanned deep space missions to the Moon and Mars.

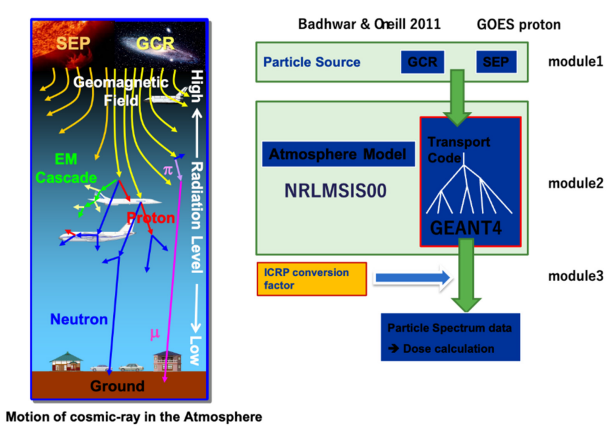

Fig. 10. Structure of the KREAM model configuration. KREAM, Korean radiation exposure assessment model.

2.4.4 Extending the Interplanetary Scintillation (IPS)-Based Solar Wind Model to Include a Longitudinal Dependence

As the solar wind expands outward, traversing the entire heliosphere up to the heliospheric boundary, it undergoes evolution over time due to various factors. One major influence is the charge-exchange interaction with neutral atoms incoming from the local interstellar medium (e.g., Gruntman et al. 2001; Lee et al. 2009). Observations by the Cassini and Interstellar Boundary Explorer (IBEX) spacecraft revealed specific structures (named "belt" and "ribbon") in energetic neutral atom images, likely produced by charge exchange interactions between solar wind ions and incoming interstellar neutral particles (Funsten et al. 2009; Krimigis et al. 2009; McComas et al. 2009; Schwadron et al. 2011; Dialynas et al. 2013). Another factor is the expansion of ICMEs over a wide longitudinal range and the merging of successive ICMEs (e.g., Burlaga 2015). The details of all such interactions and evolutions depend on the helio-latitude and helio-longitude. The specific states of solar wind speed and dynamic pressure are critical factors in addressing the spatial dependence of these interactions and evolutions (Yoo et al. 2023). Given the limited in situ measurements of solar wind, modeling solar wind parameters becomes essential. One current comprehensive model is based on the reconstruction of solar wind speed and density from interplanetary scintillation (IPS) observations (Sokół et al. 2015; Porowski et al. 2022). Fig. 11 provides an example from IPS predictions of solar wind speed and density in the ecliptic plane compared with OMNI observational data (data for all other latitudes are available, although not shown here). However, a non-negligible discrepancy with the actual OMNI observational data exists, and a contributing factor could be the absence of longitudinal dependence in this model. In situ measurements at L4 and L5 cover 1/3 of the whole longitudinal range, providing a valuable dataset for advancing the solar wind model at 1 AU.

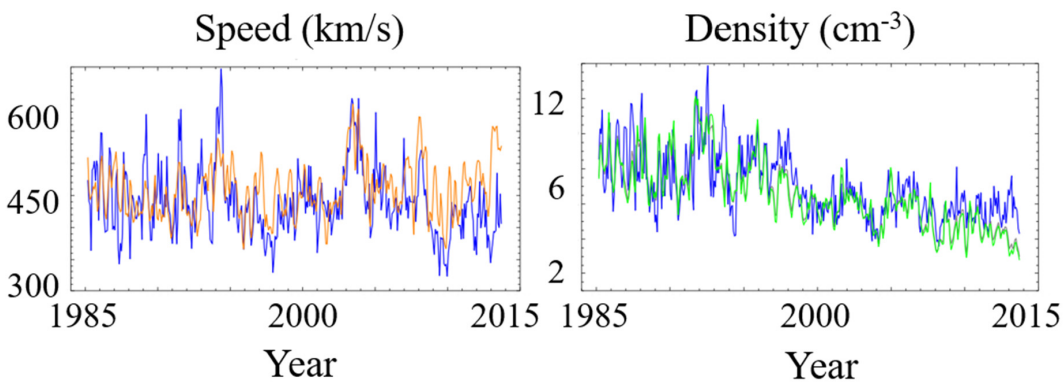

Fig. 11. Comparison of the solar wind speed and density (averaged over Carrington rotations) between the OMNI database values (blue lines) and the IPS model predictions (the other colors) in the ecliptic plane reproduced utilizing the model by Sokół et al. (2015). Adapted from Sokół et al. (2015) with CC-BY. IPS, interplanetary scintillation.

3. SUMMARY AND FINAL REMARKS

As of this writing, the Korean heliospheric science community is actively exploring the feasibility of placing a spacecraft at L4, with the expectation of reaching a conclusion in the very near future. This initiative is likely to take the form of international collaboration, with similar missions anticipated at L5 and L1. The L4 spacecraft is envisioned to carry a suite of in situ measurement instruments complemented by remote sensing instruments. In this article, we aim to identify promising science topics that can primarily leverage in situ observations at L4, alongside those at L1 and L5. Anticipating the launch of the L4 mission spacecraft in 10 years or later, our focus has been on long-term science topics. While remaining open to other topics that may emerge in the future, we propose analyzing the following science topics:

1. CME acceleration and deceleration, CME-CME interaction, CME-solar wind interaction, and CME structure (particularly longitudinal structure)
2. Structure and origin of small-scale flux ropes in contrast to typical magnetic clouds
3. Comparison of the structure of HCSs for different Lagrange points and different radial distances
4. Interplanetary field line structure and current sheets: Distinguishing solar magnetic field polarity sector boundaries from HCSs with electron strahl beams
5. Spatial and temporal characteristics of SEPs with a distinction between flare-associated and CME-associated SEPs
6. Kinetic plasma waves and instabilities, their interaction physics, coupling to large-scale structure and solar wind expansion, and their spatial dependence
7. Type III and type II solar radio bursts associated with gradual and impulsive SEPs as early warning indicators of energetic events and testbeds for nonlinear plasma physics
8. Improvement of models for CME evolution and particle acceleration using continuous multi-point in situ observations
9. Advanced modeling of small-scale flux ropes using multi-Lagrange point observations and comparisons among different modeling techniques
10. Advancement of the Korean Radiation Exposure Assessment Model for the aviation route dose (KREAM) model by extending the prediction capability to longer-term prediction times and to low Earth orbit
11. Advanced reconstruction of solar wind speed and density from IPS observations by including a longitudinal dependence

By integrating in-situ observation-based topics with other scientific areas derived from remote sensing observations, we anticipate making a substantial contribution to the progress of the inner heliospheric science field. Moreover, establishing a network for international collaborative research would be advantageous for investigating these research topics. As the Korean heliospheric science community approaches a determination on the feasibility of the L4 mission, this research paper serves as a robust roadmap, laying the foundation for meaningful contributions to the field in the years ahead.

ACKNOWLEDGMENTS

Dae-Young Lee acknowledges support from the National Research Foundation of Korea under grant NRF-2019 R1A2C1003140. This work was also supported by the Korea Astronomy and Space Science Institute under the R&D program (2024E90100). The work of K.-E.C. was supported by NASA grants 80NSSC22K0433, 80NSSC22K0522, and NASA's Living with a Star (LWS) program (contract 80NSSC20 K0218). The work of K.R. was partly supported by the National Research Foundation of Korea under grant NRF-2021M1A3 A4A06086639. Wilcox Solar Observatory data used in this study was obtained via the web site http://wso.stanford.edu at 2024:03:04_21:40:59 PST courtesy of J.T. Hoeksema.

ORCIDs

Dae-Young Lee	https://orcid.org/0000-0001-9994-7277
Rok-Soon Kim	https://orcid.org/0000-0002-9012-399X
Kyung-Eun Choi	https://orcid.org/0000-0003-2054-6011
Jungjoon Seough	https://orcid.org/0000-0002-1723-5944
Junga Hwang	https://orcid.org/0000-0002-6862-5854
Dooyoung Choi	https://orcid.org/0000-0002-3393-9060
Ji-Hyeon Yoo	https://orcid.org/0000-0002-2081-076X
Seunguk Lee	https://orcid.org/0000-0001-8045-6398
Sung Jun Noh	https://orcid.org/0000-0002-8032-7833
Jongho Seon	https://orcid.org/0000-0001-6952-656X
Kyung-Suk Cho	https://orcid.org/0000-0003-2161-9606
Kwangsun Ryu	https://orcid.org/0000-0001-8550-4213
Khan-Hyuk Kim	https://orcid.org/0000-0001-8872-6065
Jong-Dae Sohn	https://orcid.org/0000-0002-6572-622X
Jae-Young Kwak	https://orcid.org/0000-0001-7143-551X
Peter H. Yoon	https://orcid.org/0000-0001-8134-3790

REFERENCES

Agapitov OV, Dudok de Wit T, Mozer FS, Bonnell JW, Drake JF, et al., Sunward-propagating whistler waves collocated with localized magnetic field holes in the solar wind: Parker Solar Probe observations at 35.7 $R_\odot$ radii, Astrophys. J. Lett. 891, L20 (2020). https://doi.org/10.3847/2041-8213/ab799c

Bale SD, Badman ST, Bonnell JW, Bowen TA, Burgess D, et al., Highly structured slow solar wind emerging from an equatorial coronal hole, Nature. 576, 237-242 (2019). https://doi.org/10.1038/s41586-019-1818-7

Blanco JJ, Rodriguez-Pacheco J, Hidalgo MA, Sequeiros J, Monitoring the heliospheric current sheet local structure for the years 1995 to 2001, J. Atmos. Sol. Terres. Phys. 70, 226-233 (2008). https://doi.org/10.1016/j.jastp.2007.08.030

Boardsen SA, Jian LK, Raines JL, Gershman DJ, Zurbuchen TH, et al., MESSENGER survey of *in situ* low frequency wave storms between 0.3 and 0.7 AU, J. Geophys. Res. 120, 10207-10220 (2015). https://doi.org/10.1002/2015JA021506

Bowen TA, Chandran BDG, Squire J, Bale SD, Duan D, et al., *In situ* signature of cyclotron resonant heating in the solar wind, Phys. Rev. Lett. 129, 165101 (2022). https://doi.org/10.1103/PhysRevLett.129.165101

Bowen TA, Mallet A, Huang J, Klein KG, Malaspina DM, et al., Ion-scale electromagnetic waves in the inner heliosphere, Astrophys. J. Suppl. Ser. 246, 66 (2020). https://doi.org/10.3847/1538-4365/ab6c65

Breneman A, Cattell C, Schreiner S, Kersten K, Wilson LB 3rd, et al., Observations of large-amplitude, narrowband whistlers at stream interaction regions, J. Geophys. Res. Space Phys. 115, A08104 (2010). https://doi.org/10.1029/2009JA014920

Burlaga L, Voyager observations of the magnetic field in the heliosheath and the local interstellar medium, J. Phys. Conf. Ser. 642, 012003 (2015). https://doi.org/10.1088/1742-6596/642/1/012003

Burlaga LF, Ness NF, Richardson JD, Heliosheath magnetic field and plasma observed by Voyager 2 during 2015 near solar maximum, Astrophys. J. 861, 9 (2018). https://doi.org/10.3847/1538-4357/aac6b8

Cattell C, Vo T, Modeling interactions of narrowband large amplitude whistler-mode waves with electrons in the solar wind inside ~0.3 AU and at 1 AU using a particle tracing code, Astrophys. J. Lett. 914, L33 (2021). https://doi.org/10.3847/2041-8213/ac08a1

Cattell CA, Short B, Breneman AW, Grul P, Narrowband large amplitude whistler-mode waves in the solar wind and their association with electrons: STEREO waveform capture observations, Astrophys. J. 897, 126 (2020). https://doi.org/10.3847/1538-4357/ab961f

Chen Y, Hu Q, Effects of radial distances on small-scale magnetic flux ropes in the solar wind, Astrophys. J. 894, 25 (2020). https://doi.org/10.3847/1538-4357/ab8294

Chen Y, Hu Q, Allen RC, Jian LK, Small-scale magnetic flux ropes in stream interaction regions from Parker Solar Probe and Wind spacecraft observations, Astrophys. J. 943, 33 (2023). https://doi.org/10.3847/1538-4357/aca894

Cho KS, Hwang J, Han JY, Choi SH, Park SH, et al., Opening new horizons with the L4 mission: vision and plan, J. Korean Astron. Soc. 56, 263-275 (2023). https://doi.org/10.5303/JKAS.2023.56.2.263

Choi D, Lee DY, Choi KE, Noh SJ, SH43D-3178 Determination of current sheet structure in the inner heliosheath using Voyager observations, AGU Annual Meeting 2023, San Francisco, CA, 11-15 Dec 2023.

Choi KE, Lee DY, Marubashi K, Lee S, Near-orthogonal orientation of small-scale magnetic flux ropes relative to the background interplanetary magnetic field, Astrophys. J. 931, 98 (2022). https://doi.org/10.3847/1538-4357/ac69d3

Choi KE, Lee DY, Noh SJ, Agapitov O, Series of small-scale low plasma β magnetic flux ropes originating from the same longitudinal region: parker solar probe observations, Astrophys. J. 961, 3 (2024). https://doi.org/10.3847/1538-4357/ad02f6

Choi KE, Lee DY, Wang HE, Lee S, Kim KC, et al., Characteristics of suprathermal electrons in small-scale magnetic flux ropes and their implications on the magnetic connection to the sun, Sol. Phys. 296, 148 (2021). https://doi.org/10.1007/s11207-021-01888-0

Cucinotta FA, Hu S, Schwadron NA, Kozarev K, Townsend LW, et al., Space radiation risk limits and Earth-Moon-Mars environmental models, Space Weather. 8, S00E09 (2010). https://doi.org/10.1029/2010SW000572

Desai M, Giacalone J, Large gradual solar energetic particle events, Living Rev. Sol. Phys. 13, 3 (2016). https://doi.org/10.1007/s41116-016-0002-5

Dialynas K, Krimigis SM, Mitchell DG, Roelof EC, Decker RB, A three-coordinate system (ecliptic, galactic, ISMF) spectral analysis of heliospheric ENA emissions using Cassini/INCA measurements, Astrophys. J. 778, 40 (2013). https://doi.org/10.1088/0004-637X/778/1/40

Drake JF, Agapitov O, Swisdak M, Badman ST, Bale SD, et al., Switchbacks as signatures of magnetic flux ropes generated by interchange reconnection in the corona, Astron. Astrophys. 650, A2 (2021). https://doi.org/10.1051/0004-6361/202039432

Foullon C, Lavraud B, Wardle NC, Owen CJ, Kucharek H, et al., The apparent layered structure of the heliospheric current sheet: multi-spacecraft observations, Sol. Phys. 259, 389-416 (2009). https://doi.org/10.1007/s11207-009-9452-4

Funsten HO, Allegrini F, Crew GB, DeMajistre R, Frisch PC, et al., Structures and spectral variations of the outer heliosphere in IBEX energetic neutral atom maps, Science. 326, 964-966 (2009). https://doi.org/10.1126/science.1180927

Gary SP, Jian LK, Broiles TW, Stevens ML, Podesta JJ, et al., Ion-driven instabilities in the solar wind: WIND observations of 19 March 2015, J. Geophys. Res. Space Phys. 121, 30-41 (2016). https://doi.org/10.1002/2015JA021935

Ginzburg VL, Zhelezniakov VV, On the possible mechanisms of sporadic solar radio emission (radiation in an isotropic plasma), Soviet Astron. 2, 653 (1958).

Gopalswamy N, Properties of interplanetary coronal mass ejections, Space Sci. Rev. 124, 145-168 (2006). https://doi.org/10.1007/s11214-006-9102-1

Gruntman M, Roelof EC, Mitchell DG, Fahr HJ, Funsten HO, et al., Energetic neutral atom imaging of the heliospheric boundary region, J. Geophys. Res. Space Phys. 106, 15767-15781 (2001). https://doi.org/10.1029/2000JA000328

Hoeksema JT, Wilcox JM, Scherrer PH, The structure of the heliospheric current sheet: 1978–1982, J. Geophys. Res. 88, 9910-9918 (1983). https://doi.org/10.1029/JA088iA12p09910

Horbury TS, Matteini L, Stansby D, Short, large-amplitude speed enhancements in the near-Sunfast solar wind, Mon. Not. R. Astron. Soc. 478, 1980-1986 (2018). https://doi.org/10.1093/mnras/sty953

Hughes HL, Benedetto JM, Radiation effects and hardening of MOS technology: devices and circuits, IEEE Trans. Nuclear Sci. 50, 500-521 (2003). https://doi.org/10.1109/TNS.2003.812928

Hwang J, Dokgo K, Choi E, Park JS, Kim KC, et al., Modeling of space radiation exposure estimation program for pilots, crew and passengers on commercial flights, J. Astron. Space Sci. 31, 25-31 (2014). https://doi.org/10.5140/JASS.2014.31.1.25

Hwang JA, Lee JJ, Cho KS, Choi HS, Rho SR, et al., Space radiation measurement on the polar route onboard the Korean commercial flights, J. Astron. Space Sci. 27, 43-54 (2010). https://doi.org/10.5140/JASS.2010.27.1.043

Jagarlamudi VK, Dudok de Wit T, Froment C, Krasnoselskikh V, Larosa A, et al., Whistler wave occurrence and the interaction with strahl electrons during the first encounter of Parker Solar Probe, Astron. Astrophys. 650, A9 (2021). https://doi.org/10.1051/0004-6361/202039808

Jagarlamudi VK, Raouafi NE, Bourouaine S, Mostafavi P, Larosa A, et al., Occurrence and evolution of switchbacks in the inner heliosphere: Parker Solar Probe observations, Astrophys. J. Lett. 950, L7 (2023). https://doi.org/10.3847/2041-8213/acd778

Jian LK, Russell CT, Luhmann JG, Strangeway RJ, Leisner JS, et al., Ion cyclotron waves in the solar wind observed by STEREO near 1 AU. Astrophys. J. 701, L105-L109 (2009). https://doi.org/10.1088/0004-637X/701/2/L105

Jokipii JR, Thomas B, Effects of drift on the transport of cosmic rays. IV. Modulation by a wavy interplanetary current sheet. Astrophys. J. 243, 1115 (1981). https://doi.org/10.1086/158675

Kim KH, Moon YJ, Cho KS, Prediction of the 1-AU arrival times of CME-associated interplanetary shocks: evaluation of an empirical interplanetary shock propagation model, J. Geophys. Res. 112, A05104 (2007). https://doi.org/10.1029/2006JA011904

Kim RS, Cho KS, Lee J, Bong SC, Park YD, A refined classification of SPEs based on the multienergy channel observations, J. Geophys. Res. Space Phys. 119, 9419-9429 (2014). https://doi.org/10.1002/2014JA020358

Kim RS, Gopalswamy N, Cho KS, Moon YJ, Yashiro S, Propagation

characteristics of CMEs associated with magnetic clouds and ejecta, Sol. Phys. 284, 77-88 (2013). https://doi.org/10.1007/s11207-013-0230-y

Krimigis SM, Mitchell DG, Roelof EC, Hsieh KC, McComas DJ, Imaging the interaction of the heliosphere with the interstellar medium from Saturn with Cassini, Science. 326, 971-973 (2009). https://doi.org/10.1126/science.1181079

Lacombe C, Alexandrova O, Matteini L, Santolík O, Cornilleau-Wehrlin N, et al., Whistler mode waves and the electron heat flux in the solar wind: cluster observations, Astrophys. J. 796, 5 (2014). https://doi.org/10.1088/0004-637X/796/1/5

Lavraud B, Fargette N, Réville V, Szabo A, Huang J, et al., The heliospheric current sheet and plasma sheet during Parker Solar Probe's first orbit, Astrophys. J. Lett. 894, L19 (2020). https://doi.org/10.3847/2041-8213/ab8d2d

Lee MA, Fahr HJ, Kucharek H, Moebius E, Prested C, et al., Physical processes in the outer heliosphere, Space Sci. Rev. 146, 275-294 (2009). https://doi.org/10.1007/s11214-009-9522-9

Lee SY, Yoon PH, Lee E, Tu W, Simulation of plasma emission in magnetized plasmas, Astrophys. J. 924, 36 (2022). https://doi.org /10.3847/1538-4357/ac32bb

Lee SY, Ziebell LF, Yoon PH, Gaelzer R, Lee ES, Particle-in-cell and weak turbulence simulations of plasma emission, Astrophys. J. 871, 74 (2019). https://doi.org/10.3847/1538-4357/aaf476

Lepping RP, Szabo A, Peredo M, Hoeksema JT, Large-scale properties and solar connection of the heliospheric current and plasma sheets: WIND observations, Geophys. Res. Lett. 23, 1199-1202 (1996). https://doi.org/10.1029/96GL00658

Liou K, Wu CC, Characteristics of the heliospheric current sheets at the sector boundaries: wind observations from 1995–2020, Astrophys. J. 920, 39 (2021). https://doi.org/10.3847/1538-4357/ac1586

Liu W, Zhao J, Wang T, Dong X, Kasper JC, et al., The radial distribution of ion-scale waves in the inner heliosphere, Astrophys. J. 951, 69 (2023). https://doi.org/10.3847/1538-4357/acd53b

MacLean DJ, Labrum NR, Solar Radiophysics (Cambridge University Press, Cambridge, 1985).

McComas DJ, Allegrini F, Bochsler P, Bzowski M, Christian ER, et al., Global observations of the interstellar interaction from the Interstellar Boundary Explorer (IBEX), Science. 326, 959-962 (2009). https://doi.org/10.1126/science.1180906

Melrose DB, Coherent emission mechanisms in astrophysical plasmas, Rev. Mod. Plasma Phys. 1, 5 (2017). https://doi.org/10.1007/s41614-017-0007-0

Melrose DB, Plasma Astrophysics, Vol. I & II (Gordon and Breach Science Publishers, New York, 1980).

Miller JA, Guessoum N, Ramaty R, Stochastic fermi acceleration in solar flares, Astrophys. J. 361, 701 (1990). https://doi.org/10.1086/169233

Moldwin MB, Phillips JL, Gosling JT, Scime EE, McComas DJ, et al., Ulysses observation of a noncoronal mass ejection flux rope: evidence of interplanetary magnetic reconnection, J. Gesophys. Res. Space Phys. 100, 19903-19910 (1995). https://doi.org/10.1029/95JA01123

Morosan DE, Zucca P, Bloomfield DS, Gallagher PT, Conditions for electron-cyclotron maser emission in the solar corona, Astron. Astrophys. 589, L8 (2016). https:// doi.org/10.1051/0004-6361/201628392

Neugebauer M, Heliospheric sector boundaries: single or multiple? J. Gesophys. Res. Space Phys. 113, A12106 (2008). https://doi.org/10.1029/2008JA013453

Odstrcil D, Modeling 3-D solar wind structure, Adv. Space Res. 32, 497-506 (2003). https://doi.org/10.1016/S0273-1177(03)00332-6

Owens MJ, Forsyth RJ, The heliospheric magnetic field, Living Rev. Sol. Phys. 10, 5 (2013). https://doi.org/10.12942/lrsp-2013-5

Pagel C, Peter Gary S, de Koning CA, Skoug RM, Steinberg JT, Scattering of suprathermal electrons in the solar wind: ACE observations, J. Gesophys. Res. Space Phys. 112, A04103 (2007). https://doi.org/10.1029/2006JA011967

Palmerio E, Lee CO, Leila Mays M, Luhmann JG, Lario D, et al., CMEs and SEPs during November–December 2020: a challenge for real-time space weather forecasting, Space Weather. 20, e2021SW002993 (2022). https://doi.org/10.1029/2021SW002993

Pomoell J, Poedts S, EUHFORIA: European heliospheric forecasting information asset, J. Space Weather Space Clim. 8, A35 (2018). https://doi.org/10.1051/swsc/2018020

Porowski C, Bzowski M, Tokumaru M, A new 3D solar wind speed and density model based on interplanetary scintillation, Astrophys. J. 259, 2 (2022). https://doi.org/10.3847/1538-4365/ac35d7

Posner A, Arge CN, Staub J, StCyr OC, Folta D, et al., A multi-purpose heliophysics L4 mission, Space Weather. 19, 1-27 (2021). https://doi.org/10.1029/2021SW002777

Raouafi NE, Matteini L, Squire J, Badman ST, Velli M, et al., Parker Solar Probe: four years of discoveries at solar cycle minimum, Space Sci. Rev. 219, 8 (2023). https://doi.org/10.1007/s11214-023-00952-4

Reames DV, Four distinct pathways to the element abundances in solar energetic particles, Space Sci. Rev. 216, 20 (2020). https://doi.org/10.1007/s11214-020-0643-5

Reames DV, Particle acceleration at the Sun and in the heliosphere, Space Sci. Rev. 90, 413-491 (1999). https://doi.org/10.1023/A:1005105831781

Reames DV, Review and outlook of solar energetic particle measurements on multispacecraft missions, Front. Astron.

Space Sci. 10, 1254266 (2023). https://doi.org/10.3389/fspas.2023.1254266

Reames DV, The two sources of solar energetic particles, Space Sci. Rev. 175, 53-92 (2013). https://doi.org/10.1007/s11214-013-9958-9

Reames DV, Kallenrode MB, Stone RG, Multispacecraft observations of solar 3He-rich events, Astrophys. J. 380, 287 (1991). https://doi.org/10.1086/170585

Richardson IG, von Rosenvinge TT, Cane HV, Christian ER, Cohen CMS, et al., >25 MeV proton events observed by the high energy telescopes on the STEREO A and B spacecraft and/or at Earth during the first ~ seven years of the STEREO mission, Sol. Phys. 289, 3059-3107 (2014). https://doi.org/10.1007/s11207-014-0524-8

Rouillard AP, Sheeley NR Jr, Cooper TJ, Davies JA, Lavraud B, et al., The solar origin of small interplanetary transients, Astrophys. J. 734, 7 (2011). https://doi.org/10.1088/0004-637X/734/1/7

Sanchez-Diaz E, Rouillard AP, Lavraud B, Kilpua E, Davies JA, *In situ* measurements of the variable slow solar wind near sector boundaries, Astrophys. J. 882, 51 (2019). https://doi.org/10.3847/1538-4357/ab341c

Schulz M, Interplanetary sector structure and the heliomagnetic equator, Astrophys. Space Sci. 24, 371-383 (1973). https://doi.org/10.1007/BF02637162

Schwadron NA, Allegrini F, Bzowski M, Christian ER, Crew GB, et al., Separation of the interstellar boundary explorer ribbon from globally distributed energetic neutral atom flux, Astrophys. J. 731, 56 (2011). https://doi.org/10.1088/0004-637X/731/1/56

Scolini C, Chané E, Temmer M, Kilpua EKJ, Dissauer K, et al., CME–CME interactions as sources of CME geoeffectiveness: the formation of the complex ejecta and intense geomagnetic storm in 2017 early September, Astrophys. J. Suppl. Ser. 247, 21 (2020). https://doi.org/10.3847/1538-4365/ab6216

Seough J, Yoon PH, Nariyuki Y, Salem C, Expanding-box quasilinear model of the solar wind, Astrophys. J. 953, 8 (2023). https://doi.org/10.3847/1538-4357/acde7d

Sheeley NR Jr, Origin of the Wang–Sheeley–Arge solar wind model, Hist. Geo Space Sci. 8, 21-28 (2017). https://doi.org/10.5194/hgss-8-21-2017

Sinclair D, Dyer J, Radiation effects and COTS parts in Smallsats, Proceedings of the 27th Annual AIAA/USU Conference on Small Satellites, Logan, UT, 10-15 Aug 2013.

Smith EJ, The heliospheric current sheet, J. Geophys. Res. Space Phys. 106, 15819-15831 (2001). https://doi.org/10.1029/2000JA000120

Sokół JM, Swaczyna P, Bzowski M, Tokumaru M, Reconstruction of helio-latitudinal structure of the solar wind proton speed and density, Sol. Phys. 290, 2589-2615 (2015). https://doi.org/10.1007/s11207-015-0800-2

Squire J, Meyrand R, Kunz MW, Arzamasskiy L, Schekochihin AA, et al., High-frequency heating of the solar wind triggered by low-frequency, Nat. Astron. 6, 715-723 (2022). https://doi.org/10.1038/s41550-022-01624-z

Stansby D, Horbury TS, Chen CHK, Matteini L, Experimental determination of whistler wave dispersion relation in the solar wind, Astrophys. J. Lett. 829, L16 (2016). https://doi.org/10.3847/2041-8205/829/1/L16

Szabo A, Larson D, Whittlesey P, Stevens ML, Lavraud B, et al., The heliospheric current sheet in the inner heliosphere observed by the *Parker Solar Probe*, Astrophys. J. 246, 47 (2020). https://doi.org/10.3847/1538-4365/ab5dac

Telloni D, Persistence of ion cyclotron waves and stochasticity of kinetic Alfvén waves in the solar wind, Atmosphere. 12, 44 (2021). https://doi.org/10.3390/atmos12010044

Telloni D, Bruno R, D'Amicis R, Pietropaolo E, Carbone V, Wavelet analysis as a tool to localize magnetic and cross-helicity events in the solar wind, Astrophys. J. 751, 19 (2012). https://doi.org/10.1088/0004-637X/751/1/19

Tong Y, Vasko IY, Artemyev AV, Bale SD, Mozer FS, et al., Statistical study of whistler waves in the solar wind at 1 au, Astrophys. J. 878, 41 (2019). https://doi.org/10.3847/1538-4357/ab1f05

Verniero JL, Larson DE, Livi R, Rahmati A, McManus MD, et al., Parker Solar Probe observations of proton beams simultaneous with ion-scale waves, Astrophys. J. Suppl. Ser. 248, 5 (2020). https://doi.org/10.3847/1538-4365/ab86af

Verscharen D, Klein KG, Maruca BA, The multi-scale nature of the solar wind, Living Rev. Sol. Phys. 16, 5 (2019). https://doi.org/10.1007/s41116-019-0021-0

Viall NM, DeForest CE, Kepko L, Mesoscale structure in the solar wind, Front. Astron. Space Sci. 8, 735034 (2021). https://doi.org/10.3389/fspas.2021.735034

Vršnak B, Forces governing coronal mass ejections, Adv. Space Res. 38, 431-440 (2006). https://doi.org/10.1016/j.asr.2005.03.090

Vršnak B, Gopalswamy N, Influence of the aerodynamic drag on the motion of interplanetary ejecta, J. Geophys. Res. Space Phys. 107, SSH 2-1-SSH 2-6 (2002). https://doi.org/10.1029/2001JA000120

Wei HY, Jian LK, Russell CT, Omidi N, Ion cyclotron waves in the solar wind, in Low-Frequency Waves in Space Plasmas, eds. Keiling A, Lee DH, Nakariakov V (John Wiley & Sons, Hoboken, 2016), 253-267.

White SM, Solar radio bursts and space weather, Asian J. Phys. 16, 189-207 (2007).

Whitman K, Egeland R, Richardson IG, Allison C, Quinn P, et al., Review of solar energetic particle prediction models, Adv. Space Res. 72, 5161-5242 (2023). https://doi.org/10.1016/

j.asr.2022.08.006

Wiedenbeck ME, Mason GM, Cohen CMS, Nitta NV, Gómez-Herrero R, et al., Observations of solar energetic particles from 3He-rich events over a wide range of heliographic longitude, Astrophys. J. 762, 54 (2013). https://doi.org/10.1088/0004-637X/762/1/54

Wiedenbeck ME, Mason GM, Gómez-Herrero R, Haggerty D, Nitta NV, et al., Observations of a ^{3}He-rich SEP event over a broad range of heliographic longitudes: results from STEREO and ACE, AIP Conf. Proc. 1216, 621-624 (2010). https://doi.org/10.1063/1.3395943

Wijsen N, Aran A, Pomoell J, Poedts S, Modelling three-dimensional transport of solar energetic protons in a corotating interaction region generated with EUHFORIA, Astron. Astrophys. 622, A28 (2019). https://doi.org/10.1051/0004-6361/201833958

Wilcox Solar Observatory, Wilcox solar observatory source surface synoptic charts (2023) [Internet], viewed 2024 Mar 4, available from: http://wso.stanford.edu

Winterhalter D, Smith EJ, Burton ME, Murphy N, McComas DJ. The heliospheric plasma sheet, J. Geophys. Res. Space Phys. 99, 6667-6680 (1994). https://doi.org/10.1029/93JA03481

Yoo JH, Lee DY, Kwon RY, SH51D-2649 Modeling energetic neutral atom responses in the inner heliosheath to fast solar wind variations, Proceedings of the AGU Annual Meeting 2023, San Francisco, CA, 11-15 Dec 2023.

Zank GP, Rice WKM, Wu CC, Particle acceleration and coronal mass ejection driven shocks: a theoretical model, J. Geosphys. Res. Space Phys. 105, 25079-25095 (2000). https://doi.org/10.1029/1999JA000455

Zhao GQ, Feng HQ, Wu DJ, Pi G, Huang J, et al., On the generation mechanism of electromagnetic cyclotron waves in the solar wind: statistical results from *WIND* observations, Astrophys. J. 871, 175 (2019). https://doi.org/10.3847/1538-4357/aaf8b8

Zhao LL, Zank GP, Adhikari L, Hu Q, Kasper JC, et al., Identification of magnetic flux ropes from Parker Solar Probe observations during the first encounter, Astrophys. J. Suppl. Ser. 246, 26 (2020). https://doi.org/10.3847/1538-4365/ab4ff1

Zheng J, Hu Q, Observational evidence for self-generation of small-scale magnetic flux ropes from intermittent solar wind turbulence, Astrophys. J. Lett. 852, L23 (2018). https://doi.org/10.3847/2041-8213/aaa3d7

Zheng J, Hu Q, Chen Y, le Roux J, Automated detection of small-scale magnetic flux ropes and their association with shocks, J. Phys. Conf. Ser. 900, 012024 (2017). https://doi.org/10.1088/1742-6596/900/1/012024